

Kinetics of Dioxygen Reduction on Gold and Glassy Carbon Electrodes in Neutral Media

Guillaume Gotti^{1,2}, Katia Fajerweg², David Evrard¹, Pierre Gros^{1,*}

¹ Université de Toulouse, UPS, INPT, Laboratoire de Génie Chimique, 118 route de Narbonne, F-31062 Toulouse, France

CNRS, Laboratoire de Génie Chimique, F-31062 Toulouse, France

² CNRS, LCC (Laboratoire de Chimie de Coordination), 205 route de Narbonne, F-31077 Toulouse, France; Université de Toulouse, UPS, INPT; LCC, F-31077 Toulouse, France

*E-mail: gros@chimie.ups-tlse.fr

Received: 3 May 2013 / Accepted: 19 September 2013 / Published: 20 October 2013

The electrochemical reduction of dioxygen (O_2) has been studied on bulk gold (Au) and glassy carbon (GC) electrodes in aqueous neutral solution close to blood ionic composition. The mechanism was found to involve two successive bielectronic steps with hydrogen peroxide (H_2O_2) as the reaction intermediate whatever the electrode material used. On Au, O_2 and H_2O_2 were reduced at close potentials. The determination of the kinetic parameters of O_2 electroreduction was thus achieved after removing the cathodic current corresponding to H_2O_2 reduction. Cyclic voltammograms exhibited one cathodic peak whose both current density (j_p) and potential (E_p) evolution as a function of potential scan rate (r) was in accordance with Randles-Sevcik and Nicholson-Shain equations, respectively. Rotating disk electrode (RDE) voltammetry was also performed and the data were analyzed using the Koutecky-Levich relationship. The effective number of electrons (n) was found to be roughly independent of the potential and close to $n = 2$ when removing H_2O_2 reduction current whereas it gradually increased up to $n = 4$ while considering the total current. The Tafel slopes allowed the cathodic transfer coefficients (βn) to be calculated in several neutral aqueous electrolytes. Values varied from 0.25 to 0.49 and were systematically higher on Au than on GC electrode. Similar results were obtained with Tafel slopes deduced from Butler-Volmer exploitation of the current-potential curves.

Keywords: oxygen reduction – neutral aqueous media – Koutecky-Levich analysis – kinetic data – hydrogen peroxide contribution

1. INTRODUCTION

The oxygen reduction reaction (ORR) has been the subject of extensive works for many years in a large range of electrochemical applications including energy storage and conversion [1], corrosion

process [2], electrosynthesis [3] or chemical [4] and biochemical [5] analysis. In the field of electrosynthesis for instance, dioxygen (O_2) may be used directly as a strong oxidant species to perform organic oxidation reactions. Alternatively it may be reduced into hydrogen peroxide (H_2O_2) which can further be used as an oxidizing, bleaching or sterilizing agent for chemical or pharmaceutical industries [6]. With respect to energetics, O_2 plays a key role in fuel cells development. Thus, many studies have been devoted to the ORR kinetics on various bulk or electrodeposited metals, platinum being the best material in acidic solution whereas gold (Au), and particularly Au(100), affords better performances in basic media [7]. Acid and basic solutions have been almost systematically used since they have been proved to minimize the ohmic resistance between electrodes, even if the recent development of microbial fuel cells has encouraged studies in neutral media [8]. In this context a lot of works dealing with the ORR mechanism have been reported in the literature [9-13]. In these numerous papers, the Damjanovic model which describes the ORR as a multi-electron reaction is often referred to [14]. Thus, O_2 may be reduced via the so-called "direct" pathway involving a four-electron transfer (equation 1) or via the "series" pathway including two successive bielectronic transfer steps (equation 2 and 3) with H_2O_2 as reaction intermediate [15-17].



The ORR is also of great importance in neutral pH, particularly in the frame of electroanalysis. Oxygen monitoring is currently performed for environment survey or analysis in clinical biology. In the former case O_2 is used as an indicator of the quality of natural water since its concentration is critical for the survival of aquatic plants and animals [18]. In biological analysis the assay of dissolved dioxygen (determined either *in vitro* or *in vivo*) is very important for medical diagnosis [19] as it is involved in many human physiological processes such as energetic metabolism and oxidative stress. The raw reaction scheme of ORR in neutral media has been investigated using cyclic voltammetry (CV) [20], rotating disk electrode (RDE) [21] and rotating ring-disk electrode (RRDE) experiments [22], or by electrochemical impedance spectroscopy (EIS) [23]. It is generally accepted that the reduction of O_2 at polycrystalline Au electrode in neutral aqueous media involves a two-electron process, leading to the formation of H_2O_2 (equation 2). The application of more cathodic potentials induces further reduction into water (equation 3). Surprisingly kinetic data in neutral aqueous media are relatively scarce. However a quantitative determination of O_2 reduction kinetics is as important as the qualitative understanding of O_2 reduction pathway. For instance Raj et al. highlighted the electrocatalytic effect of nano-sized gold particles stabilized on bare gold electrode by using disulfide and an aromatic dithiol towards ORR in phosphate buffer solution (PBS) (pH 7.2) by CV [20]. Kuang et al. studied the ORR in 3.5 % NaCl solution on glassy carbon (GC) by means of EIS [23]. Unfortunately no kinetic study was provided in these two works. More recently a significantly enhanced catalytic activity of both bulk Au and Au nanoparticles towards ORR in PBS (pH 7.4) by means of repetitive potential cycling was reported [24]. A Cu(II)/Cu(I) complex of 1,10-phenanthroline was shown to produce a similar catalytic effect on GC electrode [25]. In both cases the

electrocatalytic activity towards the four-electron O_2 reduction was demonstrated but no transfer coefficient was determined. Finally a specific study of catalase-catalyzed ORR on GC electrode has been performed in PBS (pH 8.0) [26]. The intrinsic reaction rate constants (k°) corresponding to the successive two-electron steps have been theoretically determined by resolving mass balance equations but this system is not under the topic of the present paper. Indeed, before investigating the actual and precise effect of several electrode modification procedures it appears to be of critical interest to have a classical but complete study of ORR kinetics in neutral media on unmodified bulk electrode materials. The aim of this paper is to investigate the ORR on Au and GC electrodes in NaCl, $NaHCO_3$ and NaCl/ $NaHCO_3$ solutions close to blood ionic composition. Steady-state and cyclic voltammetry were used to exhibit the respective contribution of O_2 and H_2O_2 reduction on the overall cathodic signal. Koutecky-Levich analysis of data obtained from RDE experiments was also performed in order the kinetic parameters of the ORR (number of electrons exchanged, cathodic transfer coefficient) to be determined.

2. MATERIAL AND METHODS

2.1. Chemicals

All the solutions were prepared using ultrapure water (Milli-Q, Millipore, 18.2 M Ω cm). 95 % H_2SO_4 (normapur grade) and 37 % HCl were supplied by VWR Prolabo. NaCl, $NaHCO_3$ and 30 % H_2O_2 (analytical grade) were obtained from Fisher Scientific. The 99 % Bovine Serum Albumin (BSA) was obtained from Sigma Aldrich.

2.2. Materials

All the electrochemical experiments were performed at 293 K in a thermostated glass cell (Metrohm). A three-electrode system was used with an μ -Autolab II potentiostat (Metrohm Autolab, Utrecht, Netherlands) interfaced to a personal computer and controlled with NOVA 1.7 software package (Metrohm). The reference electrode was a Metrohm Ag/AgCl/KCl saturated electrode separated from the electrochemical cell by a Teflon PTFE capillary containing the electrolytic solution. A Metrohm glassy carbon (GC) wire was used as counter electrode. Working electrodes were a 2 mm diameter ($A = 3.142 \text{ mm}^2$) gold (Au) and a 3 mm diameter ($A = 7.069 \text{ mm}^2$) GC rotating disk electrodes (RDE) from Radiometer.

2.3. Electrode preparation

Prior to electrochemical measurements, GC surfaces were polished successively by silicon carbide grinding paper (grit 1200) for 20 s, and by a 9 μm , 3 μm , 1 μm and 1/4 μm diamond powder (Presi) on a cloth polishing pad for 2 min. Au electrodes were polished successively by a silicon carbide grinding paper (grit 1200) for 10 s, and by 5 μm , 1 μm and 0.3 μm alumina slurry during 2

min. Between each polishing step, the electrodes were thoroughly rinsed with ultrapure water and then cleaned three times in an ultrasonic ethanol bath for 5 min. The electrode surface quality was finally controlled by using a Nikon Eclipse LV150 optical microscope. For adsorption studies, Au electrode was dipped in 1 g L^{-1} Bovine serum albumin (BSA) during 15 min, then rinsed with water and dried under nitrogen stream.

2.4. Electrochemical activation

Au electrode was electrochemically activated by cyclic voltammetry in $0.5\text{ M H}_2\text{SO}_4$ solution [27,28]. The solution was previously deaerated by bubbling nitrogen (N_2) during 10 min and a gas stream was maintained over the solution during the experiment. The potential was scanned between 0.0 V and 1.5 V at a scan rate of 100 mV s^{-1} until obtaining reproducible voltammograms. This activation process was not adopted for GC electrodes in order to avoid the formation of phenolic and/or carboxyl and/or carbonyl groups on the electrode surface [29].

2.5. Electrochemical measurements

The ORR kinetics was studied by plotting steady-state current-potential curves in aerated aqueous solutions. The potential was scanned from the open circuit potential (ocp) to H_2 evolution at a scan rate of 1 mV s^{-1} . Both boundary potentials depended on the electrolyte composition and the electrode substrate (see section 3.1). The RDE rate was maintained constant at 1500 rpm unless indicated otherwise. The solution was deaerated during 10 min and a N_2 stream was maintained over the solution to record the residual current. Linear sweep voltammograms were also recorded at various potential scan rates to better characterize ORR and to quantify the contribution of H_2O_2 reduction with respect to the whole cathodic current.

3. RESULTS AND DISCUSSION

3.1. Steady-state voltammetry of ORR

Figure 1 shows the steady-state current-potential curves recorded at Au electrode in various aqueous media. In $0.5\text{ mol L}^{-1}\text{ H}_2\text{SO}_4$ (pH 0.3) a single cathodic wave corresponding to O_2 reduction was obtained with half-wave potential $E_{1/2}$ close to 0.00 V (Figure 1, curve a). Unsurprisingly H_2 evolution appeared at relatively high potential, ca. -0.30 V . Comparatively two well-defined cathodic plateau attributed to O_2 and H_2O_2 reductions were recorded in basic $0.1\text{ mol L}^{-1}\text{ NaOH}$ solution (pH 11.6) with $E_{1/2}$ close to -0.15 V and -0.90 V , respectively (Figure 1, curve b). Deaeration of the solution resulted in a complete disappearance of both cathodic waves (Figure 1, curve c) and only the reduction of the solvent remained observed (for the sake of clarity only the curve recorded at basic pH is plotted).

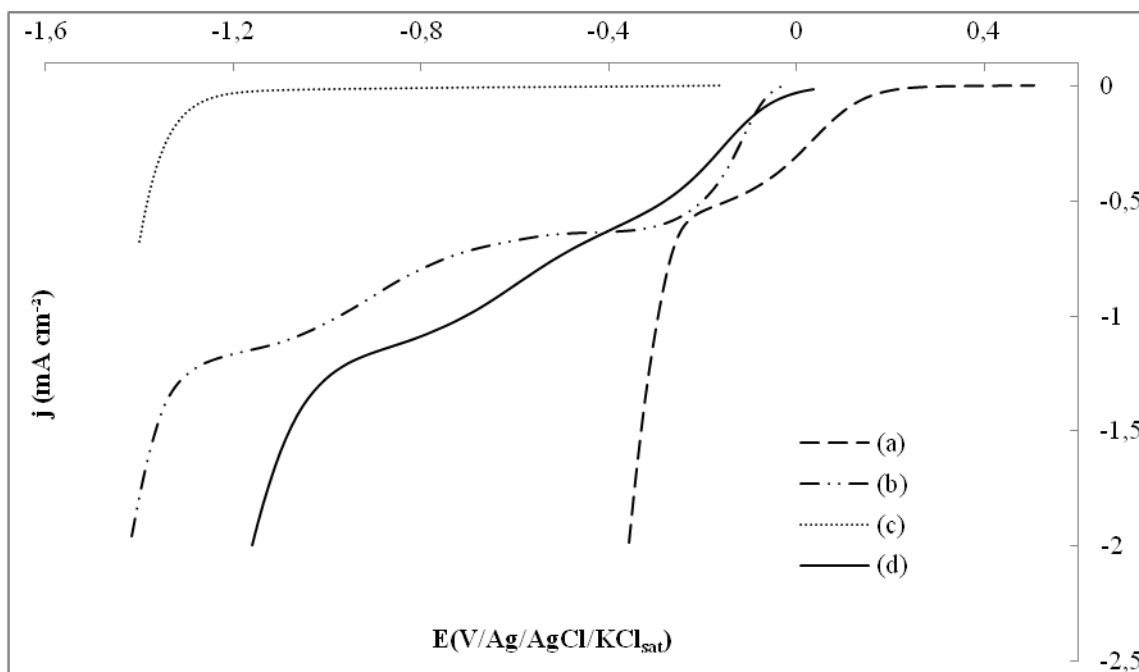


Figure 1. Steady-state current-potential curves obtained with Au RDE in: (a) 0.5 mol L⁻¹ H₂SO₄ pH 0.3; (b) aerated and (c) deaerated 0.1 mol L⁻¹ NaOH pH 11.6; (d) NaCl-NaHCO₃ (0.15 mol L⁻¹ / 0.028 mol L⁻¹ – pH 7.4). Potential scan rate: 1 mV s⁻¹; Electrode rotation rate: 1500 rpm.

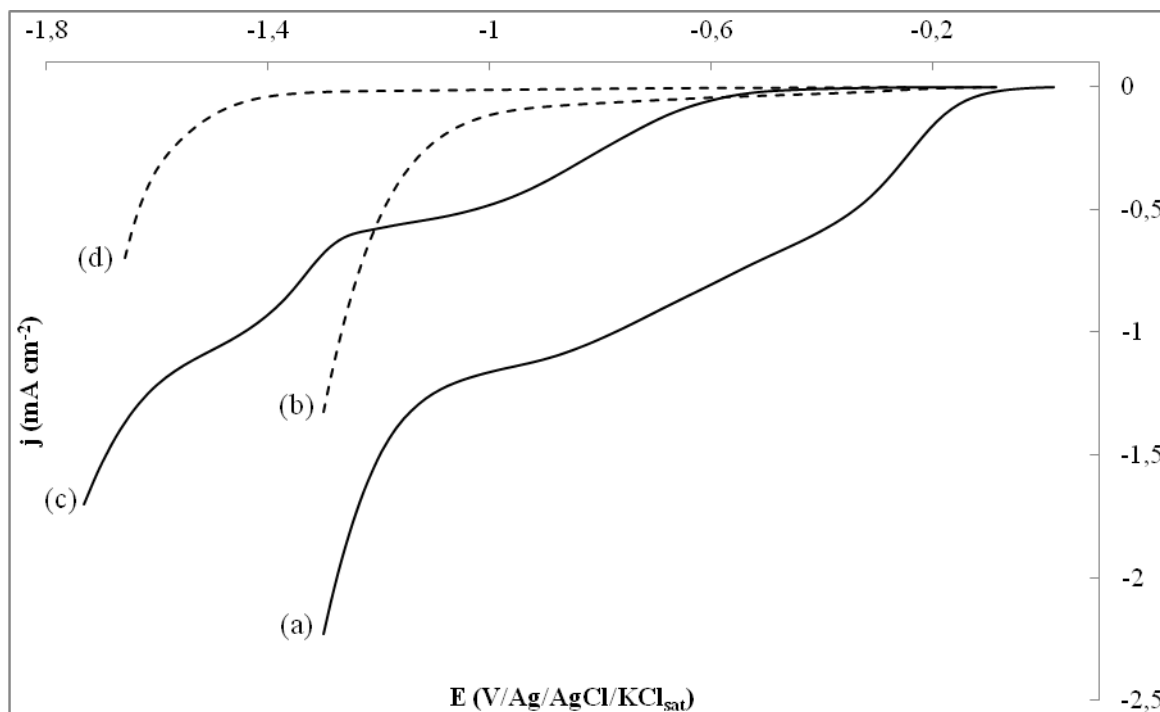


Figure 2. Steady-state current-potential curves recorded in aerated NaCl-NaHCO₃ (0.15 mol L⁻¹ / 0.028 mol L⁻¹ – pH 7.4) with: (a) Au and (c) GC RDE. (b) and (d): same experiments performed in deaerated solution. Potential scan rate: 1 mV s⁻¹; Electrode rotation rate: 1500 rpm.

All these results are in accordance with previous works [30-32]. It is noteworthy that the ORR was selective in both media, because either H_2O_2 reduction was not observed in acid solution (Figure 1, curve a) or both O_2 and H_2O_2 reduction took place at distinct potentials for high pH values (Figure 1, curve b). On the contrary in neutral $\text{NaCl}/\text{NaHCO}_3$ solution (pH 7.4) the limiting current corresponding to the bielectronic O_2 reduction was not so clear since H_2O_2 reduction began at higher potentials than previously, ca. -0.40 V (Figure 1, curve d).

Figure 2 compares the steady-state current-potential curves obtained in the latter solution on Au (Figure 2, curve a) and on GC (Figure 2, curve c) disk electrodes. Contrary to what was observed on Au, both O_2 and H_2O_2 reduction reactions occurred at sufficiently distinct potentials on GC electrode with $E_{1/2}$ close to -0.85 V and -1.35 V, respectively. These differences clearly result from the heterogeneous electronic transfer kinetics of ORR on both electrode materials. Finally no significant current was recorded in deaerated solution whatever the electrode material used (Figure 2, curves b and d).

3.2. H_2O_2 reduction contribution

O_2 and H_2O_2 being reduced at close potentials on Au electrode in neutral solution, it is important to study the electrochemical kinetics of these two species separately. In this way linear sweep voltammograms were plotted in $\text{NaCl}/\text{NaHCO}_3$ solution (pH 7.4) without (Figure 3, curve a) and with $0.24 \text{ mmol L}^{-1} \text{H}_2\text{O}_2$ (Figure 3, curve c).

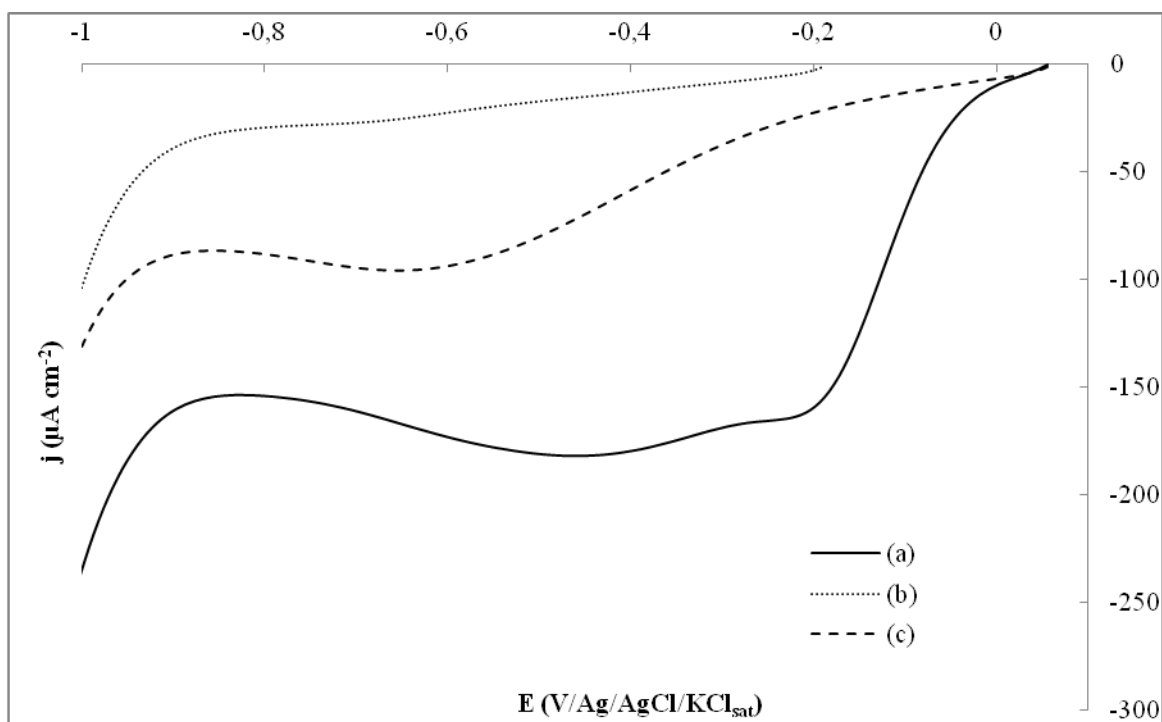


Figure 3. Linear sweep voltammograms recorded with Au electrode in: (a) aerated and (b) deaerated $\text{NaCl}/\text{NaHCO}_3$ ($0.15 \text{ mol L}^{-1} / 0.028 \text{ mol L}^{-1}$ – pH 7.4) solution. (c) Same deaerated solution containing $0.24 \text{ mmol L}^{-1} \text{H}_2\text{O}_2$. Potential scan rate: 50 mV s^{-1} .

This concentration was chosen in order the H_2O_2 reduction reaction rate to be close to that actually occurring during the two successive two-electron reduction steps of dioxygen. It is noteworthy that both situations are not exactly the same: in the latter case the reaction implies H_2O_2 diffusion in the bulk solution whereas in the former case H_2O_2 is produced at the Au electrode surface. Anyway Figure 3 shows that a small but significant cathodic current corresponding to H_2O_2 reduction has to be considered in the potential range where O_2 is reduced into H_2O_2 , i.e. between 0.10 V and -0.30 V.

As the aim of this work is to determine and compare the ORR kinetics on both Au and GC electrodes in neutral media, it seems essential from these previous results to remove the current corresponding to H_2O_2 reduction from the current-potential curve recorded on Au electrode in aerated $\text{NaCl}/\text{NaHCO}_3$ solution (pH 7.4). Figure 4.A shows the resulting linear sweep voltammograms obtained after subtraction of H_2O_2 reduction current for potential scan rates ranging from 25 to 200 mV s^{-1} . All the curves highlighted a main cathodic current peak corresponding to O_2 reduction only. The plots of the current density j_p recorded at potential close to -0.23 V as a function of the square root of scan rate exhibited a linear behavior with good correlation coefficients (Figure 4.B), thus satisfying the Randles-Sevcik relationship (equation 4) and being consistent with a diffusion-controlled electrochemical reaction involving an irreversible system [33]:

$$j_p = -(2.99 \times 10^5) n^{3/2} \beta^{1/2} D^{1/2} r^{1/2} C \quad (4)$$

where n is the total number of electrons transferred, β is the cathodic transfer coefficient, D is the diffusion coefficient ($1.96 \times 10^{-5} \text{ cm}^2 \text{ s}^{-1}$) [34,35], C is the dioxygen bulk concentration ($0.24 \times 10^{-6} \text{ mol cm}^{-3}$ at atmospheric pressure) [36] and r is the potential scan rate (V s^{-1}).

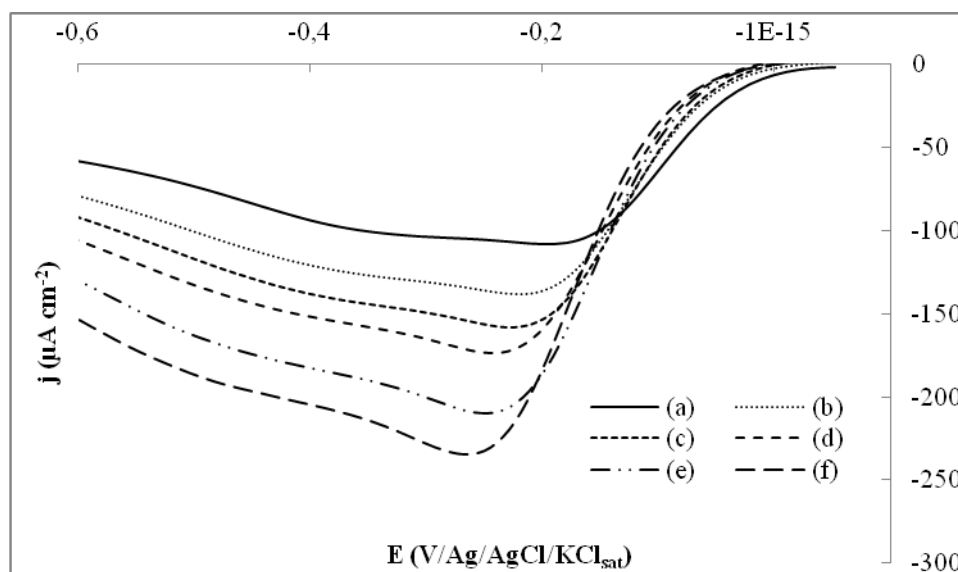


Figure 4A. Linear sweep voltammograms recorded with Au electrode in aerated NaCl/HCO_3 ($0.15 \text{ mol L}^{-1} / 0.028 \text{ mol L}^{-1} - \text{pH } 7.4$) solution. Variation of the potential scan rate: (a) 25 mV s^{-1} ; (b) 50 mV s^{-1} ; (c) 75 mV s^{-1} ; (d) 100 mV s^{-1} ; (e) 150 mV s^{-1} and (f) 200 mV s^{-1} . The curves were obtained after subtraction of the cathodic current obtained with the same deaerated solution containing $0.24 \text{ mmol L}^{-1} \text{ H}_2\text{O}_2$.

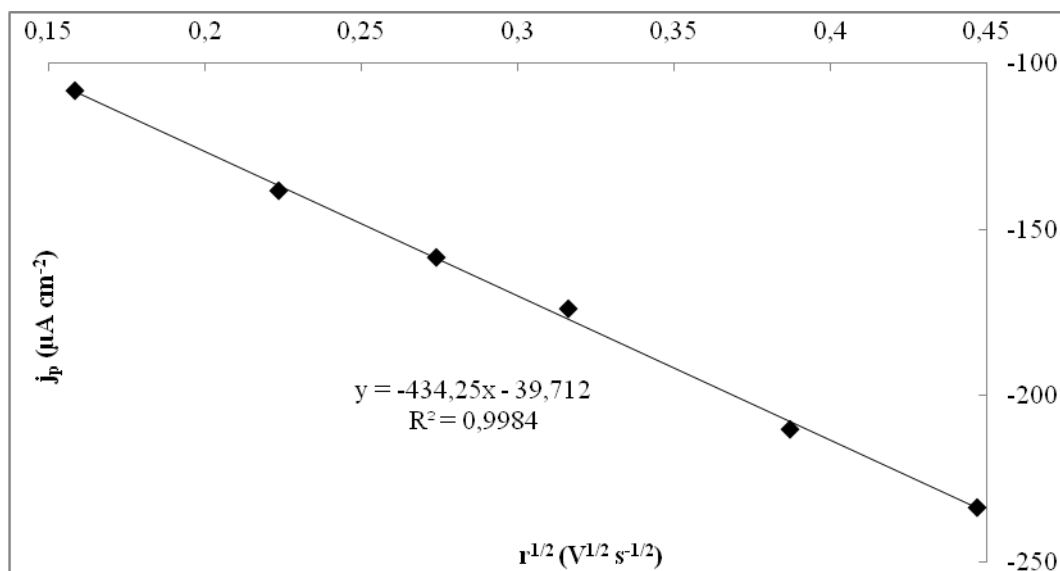


Figure 4B. Variation of current density of the ORR recorded at a potential close to -0.23 V/(Ag/AgCl/KCl_{sat}) as a function of the square root of the potential scan rate.

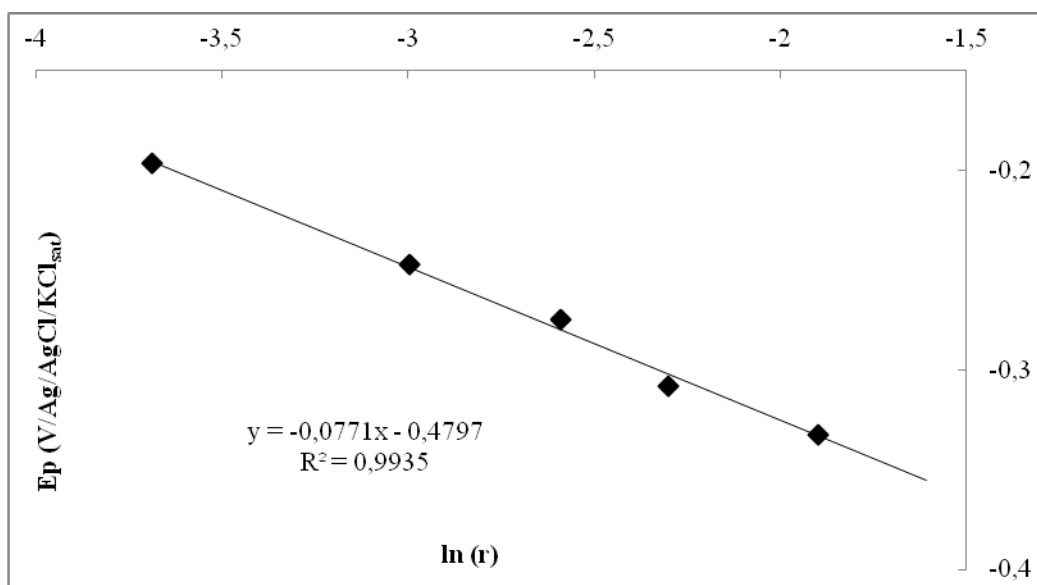


Figure 4C. Variation of the peak potential of the ORR with the natural logarithm of potential scan rate (expressed in V s⁻¹).

The corresponding peak potential E_p was found to be dependent on the natural logarithm of the potential scan rate (Figure 4.C). This is in agreement with Nicholson-Shain relation for an irreversible electrochemical system [33] (equation 5):

$$E_p = E^{*'} - \frac{RT}{\beta n F} \left[0.780 + \ln \left(\frac{D^{1/2}}{k^2} \right) + \ln \left(\frac{\beta n F r}{RT} \right)^{1/2} \right] \tag{5}$$

where E° (V) is the apparent standard potential, R is the gas constant ($8.314 \text{ J K}^{-1} \text{ mol}^{-1}$), T is the temperature (K), F is the Faraday constant (96500 C mol^{-1}) and k° (cm s^{-1}) is the intrinsic heterogeneous transfer rate constant. The same evolutions were obtained using a GC electrode (not shown): the only difference was that the reduction peak was observed at higher cathodic overpotential in accordance with results shown in Figure 2.

It was also found that the plot of j_p recorded with Au electrode as a function of scan rate was close to linearity, suggesting that part of the reduction process may be due to O_2 adsorbed onto Au surface (not shown). To support this hypothesis, the same linear voltammograms were recorded with Au modified with BSA (see section 2.3). In this latter case only the plot of j_p as a function of the square root of scan rate exhibited a linear trend. However the adsorption step was not energetically prevalent since only one single cathodic peak was observed in all the voltammograms.

3.3. ORR kinetics determination

Figure 5.A shows the steady-state current-potential curves recorded on Au RDE in $\text{NaCl}/\text{NaHCO}_3$ solution (pH 7.4) at different rotation rates ω ranging from 500 to 3000 rpm. In the potential range from the ocp to around -0.15 V the current did not depend on the rotation rate since the charge transfer is the reaction rate limiting step. At potentials lower than -0.15 V , the current increased while increasing the rotation rate. However the current plateau corresponding to mass transfer limitation was not completely defined. This makes evidence that the ORR results from a mixed kinetic-diffusion control mechanism as shown in Figure 1.

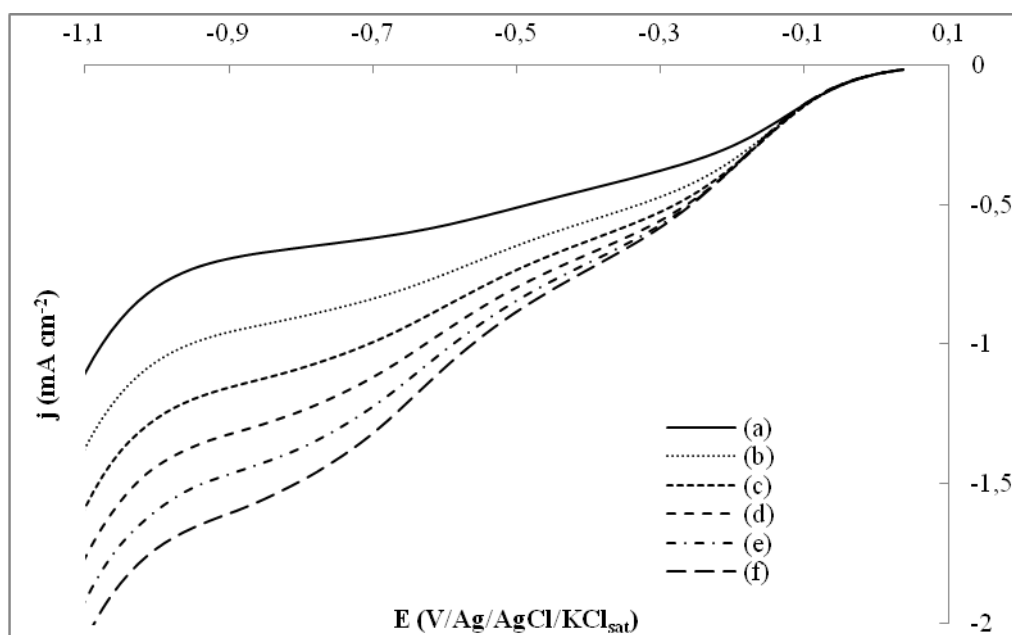


Figure 5A. Steady-state current-potential curves recorded with Au RDE in aerated NaCl/HCO_3 ($0.15 \text{ mol L}^{-1} / 0.028 \text{ mol L}^{-1} - \text{pH } 7.4$) solution. Variation of the rotating disk rate: (a) 500 rpm; (b) 1000 rpm; (c) 1500 rpm; (d) 2000 rpm; (e) 2500 rpm and (f) 3000 rpm. Potential scan rate: 1 mV s^{-1} .

To go further into detail the data were analyzed by means of the Koutecky-Levich relation [37]:

$$\frac{1}{j} = \frac{1}{j_k} + \frac{1}{j_d} = -\frac{1}{nFkC} - \frac{1}{0.62nFD^{2/3}\omega^{1/2}\nu^{-1/6}\epsilon_C} \quad (6)$$

where j_k and j_d are the kinetic limited and mass transfer controlled current densities, respectively, k is the potential-dependent charge transfer rate constant and ν is the kinematic viscosity of the aqueous solution ($0.01 \text{ cm}^2 \text{ s}^{-1}$) [38]. According to equation (6) the inverse of the current density $1/j$ was plotted as a function of the inverse of the square root of the rotation rate. Figure 5.B highlighted that linear variations were obtained for potentials ranging from -0.10 V to -0.36 V which correspond to the ORR.

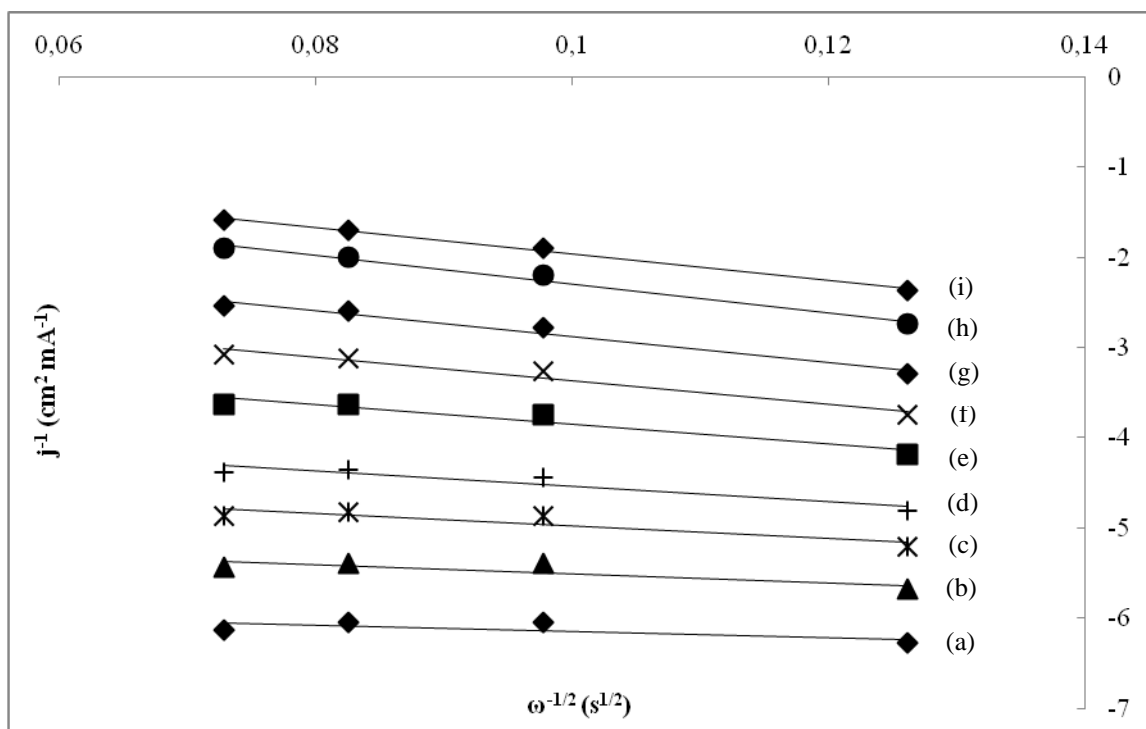


Figure 5B. Koutecky-Levich plots at different potentials (V/(Ag/AgCl/KCl_{sat})) : (a) -0.10; (b) -0.11; (c) -0.12; (d) -0.13; (e) -0.15; (f) -0.17; (g) -0.20; (h) -0.28 and (i) -0.36.

The slope of each straight line allowed the total number of electron to be determined. Figure 5.C (curve ■) reports the resulting values as a function of the Au electrode potential. For potential higher than -0.40 V the number of electrons was found to be close to $n = 2$. This is in agreement with previous studies showing the reduction of O_2 into H_2O_2 on polycrystalline Au [39-41]. Calculations were also performed for potentials ranging from -0.36 V to -1.00 V where H_2O_2 is further reduced into H_2O as indicated in Figure 5.A. The number of electrons gradually increased up to $n = 4$ while decreasing the potential (values of n higher than 4 certainly result from the simultaneous reduction of water starting at potential close to -0.95 V as shown in Figure 5.A).

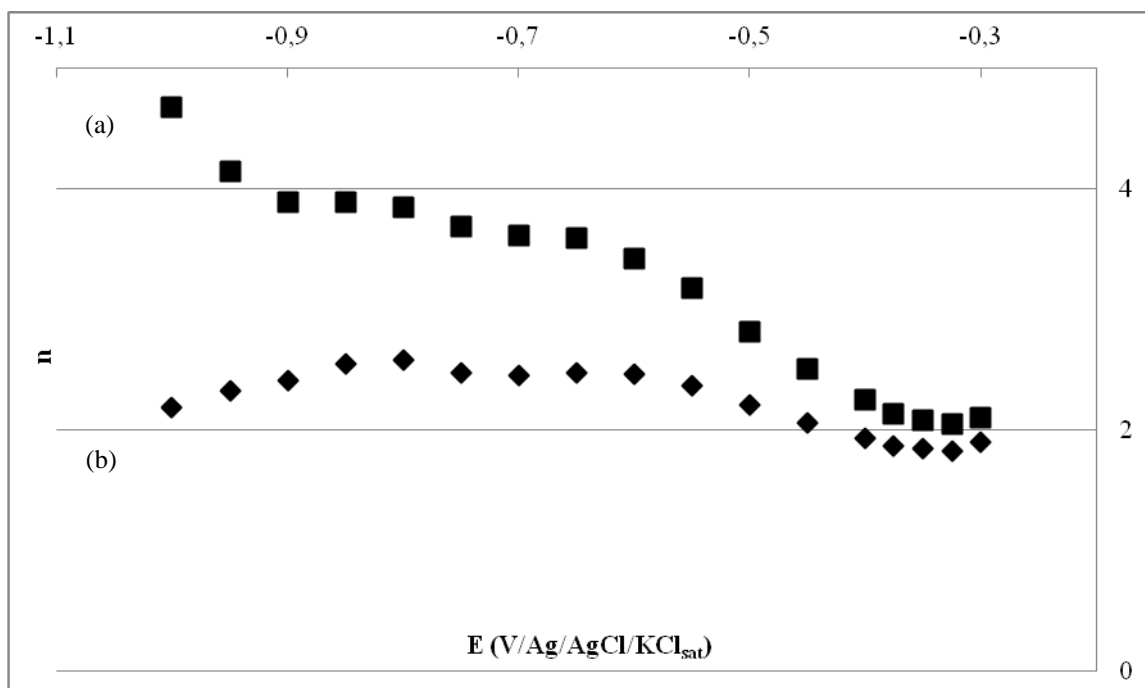


Figure 5C. Variation of the number of electrons involved in the ORR with the Au electrode potential. (a) Values deduced from the current-potential curves recorded in the aerated NaCl/NaHCO₃ (0.15 mol L⁻¹ / 0.028 mol L⁻¹ – pH 7.4) solution (as in Fig 5A.); (b) Values obtained after subtraction of the cathodic current obtained with the same deaerated solution containing 0.24 mmol L⁻¹ H₂O₂.

Calculations were also done from the current-potential curves recorded on Au RDE in NaCl/NaHCO₃ solution (pH 7.4) and plotted after removing the current corresponding to the reduction of 0.24 mmol L⁻¹ H₂O₂ (curves not shown). In this latter case the number of electron remained roughly constant and close to $n = 2$ (Figure 5.C, curve \blacklozenge). It is noteworthy that n was slightly higher than 2 in the potential range from -0.55 V to -0.90 V. We believe that this discrepancy did not result from a complex reduction mechanism but is rather due to the imperfect subtraction of the H₂O₂ reduction current. Anyway the two curves shown in Figure 5.C are significantly different, thus highlighting the contribution of H₂O₂ reduction in the global amperometric signal [42,43]. The intercepts of the Koutecky-Levich plots (Figure 5.B) allowed the kinetic limited current densities j_k to be determined. These latter were plotted (natural logarithm scale) in Figure 5.D as a function of the electrode potential (curve a). A similar curve was obtained from the current-potential curves without H₂O₂ reduction current (Figure 5.D, curve b). Both curves resulted in a linear correlation with similar Tafel slopes. The corresponding cathodic transfer coefficient βn were calculated from the charge transfer rate constant k (equation 7):

$$k = k^{\circ} \exp\left(-\frac{\beta n F}{RT}(E - E^{\circ'})\right) \quad (7)$$

where k° (cm s⁻¹) is the intrinsic charge transfer rate constant. The values were 0.36 and 0.33, respectively. Considering the number of electrons exchanged for the ORR in the same potential range

obtained from Figure 5.C (2.1 and 1.9, respectively), both cathodic transfer coefficients β were found to be very similar and close to 0.17.

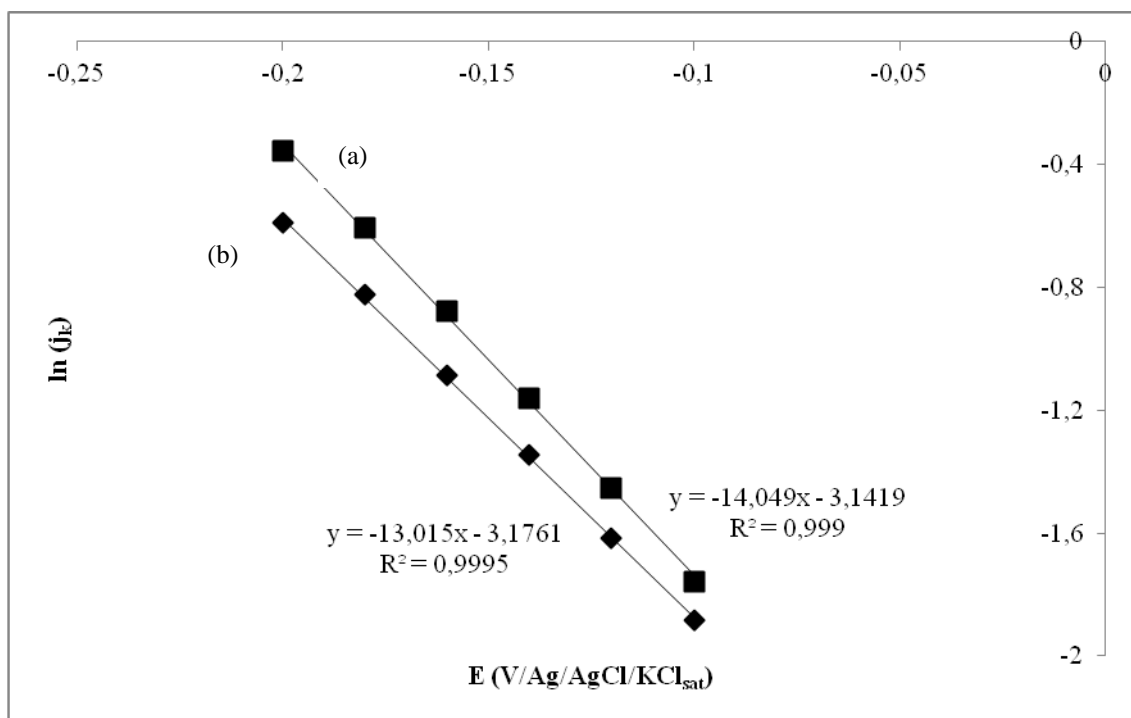


Figure 5D. Variation of the kinetic limited current density (expressed in mA cm^{-2}) of the ORR with the Au electrode potential. (a) Values deduced from the current-potential curves recorded in the aerated $\text{NaCl}/\text{NaHCO}_3$ ($0.15 \text{ mol L}^{-1} / 0.028 \text{ mol L}^{-1} - \text{pH } 7.4$) solution (as in Fig 5A.); (b) Values obtained after subtraction of the cathodic current obtained with the same deaerated solution containing $0.24 \text{ mmol L}^{-1} \text{ H}_2\text{O}_2$.

Table 1. Values of cathodic transfer coefficient β_n obtained with Au and GC electrodes in several neutral aqueous electrolytes.

Bulk gold electrode												
Conditions	NaCl $0.1 \text{ mol L}^{-1} - \text{pH } 6.2$		NaHCO ₃ $0.028 \text{ mol L}^{-1} - \text{pH } 6.2$		NaCl-NaHCO ₃ $0.2 \text{ mol L}^{-1} / 0.028 \text{ mol L}^{-1} - \text{pH } 6.5$			NaCl-NaHCO ₃ $0.15 \text{ mol L}^{-1} / 0.028 \text{ mol L}^{-1} - \text{pH } 7.4$				
Tafel	0.43	± 0.02	0.46	± 0.02	0.49	± 0.01	0.39	± 0.03				
Koutecky-Levich	0.34	± 0.07	0.47	± 0.04	0.49	± 0.01	0.38	± 0.01				
Average	0.39	± 0.05	0.47	± 0.03	0.49	± 0.01	0.39	± 0.02				
Glassy carbon electrode												
Conditions	NaCl $0.1 \text{ mol L}^{-1} - \text{pH } 6.2$		NaHCO ₃ $0.028 \text{ mol L}^{-1} - \text{pH } 6.2$		NaCl-NaHCO ₃ $0.2 \text{ mol L}^{-1} / 0.028 \text{ mol L}^{-1} - \text{pH } 6.5$			NaCl-NaHCO ₃ $0.15 \text{ mol L}^{-1} / 0.028 \text{ mol L}^{-1} - \text{pH } 7.4$				
Tafel	0.30	± 0.01	0.31	± 0.01	0.27	± 0.01	0.25	± 0.02				
Koutecky-Levich	0.28	± 0.02	0.30	± 0.01	0.25	± 0.02	0.23	± 0.01				
Average	0.29	± 0.02	0.30	± 0.01	0.26	± 0.01	0.24	± 0.02				

It might thus be concluded that the contribution of H₂O₂ reduction in the ORR kinetics is not so important and may be finally neglected in a first approach. The same experiments were performed with other neutral aqueous electrolytes as well as on GC electrode (not shown). All β_n coefficient values were calculated in a similar way and are reported in Table 1. For all experimental conditions the measurements were repeated three times. The results were quite reproducible, the standard deviation being lower than 8 %. Whatever the electrolyte chosen, the cathodic transfer coefficient for ORR was found to be systematically higher on Au than on GC electrode (the average values being 0.43 and 0.27, respectively). The difference was not negligible and reached at least 17 % in 0.1 mol L⁻¹ NaCl (pH 6.2).

In order to confirm all these results, kinetic parameters were also determined by means of Tafel slopes deduced from the cathodic part of the Butler-Volmer relation [44,45] (equation 8):

$$j = j^{\circ} \left\{ \left(1 - \frac{j}{j_{l,a}} \right) \exp\left(\frac{\alpha n F}{RT} \eta\right) - \left(1 - \frac{j}{j_{l,c}} \right) \exp\left(\frac{-\beta n F}{RT} \eta\right) \right\} \quad (8)$$

where j° corresponds to the exchange current density. In the potential range studied (from -0.03 to -0.13 V) the anodic part of the current may be neglected so that only the cathodic component was considered. After recombination, the relation can be written as (equation 9):

$$\ln\left(\frac{j_{l,c} \times j}{j - j_{l,c}}\right) = \ln j^{\circ} - \frac{\beta n F}{RT} \eta \quad (9)$$

The corresponding β_n are also indicated in Table 1. All results were in accordance with previous data from Koutecky-Levich analysis, except that obtained on Au electrode in 0.1 mol L⁻¹ NaCl solution (pH 6.2) (0.43 and 0.34, respectively).

4. CONCLUSION

The electrochemical reduction of O₂ has been investigated in several aqueous neutral electrolytes both on Au and GC electrodes. O₂ and H₂O₂ being reduced at close potentials on Au, the contribution of the H₂O₂ reduction on the global current has been subtracted in order to consider O₂ reduction kinetics only. From RDE studies the number of electrons involved as well as the cathodic transfer coefficient β_n have been calculated by means of Koutecky-Levich analysis. The results were in agreement with those obtained from the exploitation of the Butler-Volmer equation. The values of β_n were higher on Au than on GC whatever the electrolyte chosen. Works are now in progress to highlight the influence of several electrode modification processes on O₂ electroreduction kinetic parameters in such neutral media.

ACKNOWLEDGMENTS

The authors thank the Pôle de Recherche et de l'Enseignement Supérieur (PRES) Toulouse and the Région Midi-Pyrénées for financial supports.

References

1. A. J. Appleby, *Fuel cell handbook*, Van Nostrand Reinhold Co. Inc., New York (1988).
2. D. Brondel, R. Edwards, A. Hayman, D. Hill, S. Mehta and T. Semerad, *Oilfield Rev.*, 6 (1994) 4.
3. J. J. Jow, A. C. Lee and T. C. Chou, *J. Appl. Electrochem.*, 17 (1987) 753.
4. B. Wang, *J. Power Sources*, 152 (2005) 1.
5. J. W. Severinghaus and P. B. Astrup, *History of Blood Gas Analysis*, Little, Brown, and Co. Inc., San Francisco (1987).
6. G. Strukul and Editor., *Catalytic Oxidations with Hydrogen Peroxide as Oxidant.*, Kluwer, Venice (1992).
7. A. Radoslav, *Recent advances in the kinetics of oxygen reduction*, Wiley-VCH, New York (1998).
8. J. Wu, Y. Wang, D. Zhang and B. Hou, *J. Power Sources*, 196 (2011) 1141.
9. R. J. Taylor and A. A. Humffray, *J. Electroanal. Chem. Interfacial Electrochem.*, 64 (1975) 63.
10. R. J. Taylor and A. A. Humffray, *J. Electroanal. Chem. Interfacial Electrochem.*, 64 (1975) 85.
11. D. T. Sawyer and E. T. Seo, *Inorg. Chem.*, 16 (1977) 499.
12. B. Sljukic, C. E. Banks, S. Mentus and R. G. Compton, *Phys. Chem. Chem. Phys.*, 6 (2004) 992.
13. K. Vaik, A. Sarapuu, K. Tammeveski, F. Mirkhalaf and D. J. Schiffrin, *J. Electroanal. Chem.*, 564 (2004) 159.
14. A. Damjanovic, M. A. Genshaw and J. O. M. Bockris, *J. Chem. Phys.*, 45 (1966) 4057.
15. D. T. Sawyer, G. Chiericato, Jr., C. T. Angelis, E. J. Nanni, Jr. and T. Tsuchiya, *Anal. Chem.*, 54 (1982) 1720.
16. E. Yeager, *Electrochim. Acta*, 29 (1984) 1527.
17. E. Yeager, *J. Mol. Catal.*, 38 (1986) 5.
18. F. King, M. J. Quinn and C. D. Litke, *J. Electroanal. Chem.*, 385 (1995) 45.
19. C. E. W. Hahn, *Analyst*, 123 (1998) 57R.
20. C. R. Raj, A. I. Abdelrahman and T. Ohsaka, *Electrochem. Comm.*, 7 (2005) 888.
21. C. Degrand, *J. Electroanal. Chem.*, 169 (1984) 259.
22. S. Strbac and R. R. Adzic, *Electrochim. Acta*, 41 (1996) 2903.
23. F. Kuang, D. Zhang, Y. Li, Y. Wan and B. Hou, *J. Solid State Electrochem.*, 13 (2009) 385.
24. J. H. Shim, J. Kim, C. Lee and Y. Lee, *J. Phys. Chem. C*, 115 (2011) 305.
25. S.-J. Liu, C.-H. Huang and C.-C. Chang, *Mater. Chem. Phys.*, 82 (2003) 551.
26. M. E. Lai and A. Bergel, *J. Electroanal. Chem.*, 494 (2000) 30.
27. D. A. J. Rand and R. Woods, *J. Electroanal. Chem. Interfacial Electrochem.*, 35 (1972) 209.
28. A. Hamelin, *J. Electroanal. Chem.*, 407 (1996) 1.
29. A. Dekanski, J. Stevanovic, R. Stevanovic, B. Z. Nikolic and V. M. Jovanovic, *Carbon*, 39 (2001) 1195.
30. J. W. Kim and A. A. Gewirth, *J. Phys. Chem. B*, 110 (2006) 2565.
31. J. Maruyama, M. Inaba and Z. Ogumi, *J. Electroanal. Chem.*, 458 (1998) 175.
32. A. J. Appleby and J. Marie, *Electrochim. Acta*, 24 (1979) 195.
33. A. J. Bard and L. R. Faulkner, *Electrochemical Methods, Fundamentals and Applications*, Masson, Paris (1982).
34. A. J. van Stroe and L. J. J. Janssen, *Anal. Chim. Acta*, 279 (1993) 213.
35. M. Jamnongwong, K. Loubiere, N. Dietrich and G. Hebrard, *Chem. Eng. J.*, 165 (2010) 758.
36. B. B. Benson and D. J. Krause, *Limnol. Oceanogr.*, 29 (1984) 620.
37. J. Koutecky, *Chem. Listy Vedu Prum.*, 47 (1953) 1758.
38. F. J. Millero, F. Huang and A. L. Laferiere, *Mar. Chem.*, 78 (2002) 217.
39. M. Alvarez-Rizatti and K. Juettner, *J. Electroanal. Chem. Interfacial Electrochem.*, 144 (1983) 351.
40. R. R. Adzic, S. Strbac and N. Anastasijevic, *Mater. Chem. Phys.*, 22 (1989) 349.
41. J. Maruyama, M. Inaba and Z. Ogumi, *J. Electroanal. Chem.*, 458 (1998) 175.

42. G. Vazquez-Huerta, G. Ramos-Sanchez, A. Rodriguez-Castellanos, D. Meza-Calderon, R. Antano-Lopez and O. Solorza-Feria, *J. Electroanal. Chem.*, 645 (2010) 35.
43. M. S. El-Deab and T. Ohsaka, *Electrochim. Acta*, 47 (2002) 4255.
44. J. Tafel, *Z. Phys. Chem.*, 34 (1900) 187.
45. J. Tafel, *Z. Phys. Chem.*, 50 (1905) 641.

© 2013 by ESG (www.electrochemsci.org)